Langmuir

Letter

pubs.acs.org/Langmuir

Maze Solving Using Fatty Acid Chemistry

Kohta Suzuno,[†] Daishin Ueyama,[†] Michal Branicki,[‡] Rita Tóth,[§] Artur Braun,[§] and István Lagzi*[,∥]

[†]Graduate School of Advanced Mathematical Sciences, Meiji University, Tokyo, Japan

[‡]School of Mathematics, University of Edinburgh, Edinburgh, U.K.

[§]Laboratory for High Performance Ceramics, Empa, Swiss Federal Laboratories for Materials Science and Technology, Dübendorf, Switzerland

[∥]Department of Physics, Budapest University of Technology and Economics, H-1111 Budapest, Budafoki út 8, Hungary

Supporting Information

ABSTRACT: This study demonstrates that the Marangoni flow in a channel network can solve maze problems such as exploring and visualizing the shortest path and finding all possible solutions in a parallel fashion. The Marangoni flow is generated by the pH gradient in a maze filled with an alkaline solution of a fatty acid by introducing a hydrogel block soaked with an acid at the exit. The pH gradient changes the protonation rate of fatty acid molecules, which translates into the surface tension gradient at the liquid−air interface through the maze. Fluid flow maintained by the surface tension gradient (Marangoni flow) can drag water-soluble dye particles toward low pH (exit) at the liquid−air interface. Dye particles placed at the entrance of the maze dissolve during this motion, thus exhibiting and finding the shortest path and all possible paths in a maze.

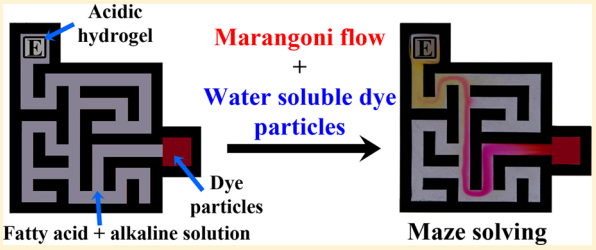

INTRODUCTION

Efficient maze solving, i.e., finding either the shortest path or all possible paths between two points in a maze, is a challenging mathematical problem especially if computational constraints are imposed. These problems can be solved using inherently slow computational methods where the solving time, t, scales with the size of the system, n, raised to some power x, i.e., $t \approx n^x$.[1,2] However, there are other possibilities such as analog computational methods that have been successfully used to solve these problems. They rely either solely on maze topology (examples include applying a pressure difference in fluid through the maze,[3] processing the path of propagating chemical waves[4] or plasma,[5] and using a network of memristors[6] and the reconfiguration of an organism between two food sources within the maze[7−9]) or on a path-finding entity (a solid hydrogel in a microfluidic network or a droplet suspended at the liquid−air interface) that can react to environmental stimuli.[10,11] In the latter example, it has been shown that a small fatty acid droplet suspended at the liquid−air interface in an alkaline solution can solve the maze and find the shortest path if a pH gradient is established in the maze.

Using the aforementioned analog computing methods can be inherently slow due to the nature of the processes used (e.g., chemical wave propagation,[4] protoplasmic tube formation[7,8,12]). Additionally, in most cases only one path (the shortest) can be explored and/or visualized. It should be mentioned that when using a memristive network all paths can be found and the maze-solving time could be short (a few nanoseconds).[6] However, chemical-based computing methods providing all possible paths through a maze are lacking and challenging.

In this letter, we will provide a new method of finding and visualizing the shortest path and all possible paths in a maze based on Marangoni flow[13−20] induced by a surface tension gradient at the liquid−air interface.[21] Specifically, we describe one such system that comprises small tracer (solid water-soluble dye) particles powered by an acid/base reaction. When subjected to a gradient of pH within a maze, these particles move toward regions of low pH and find the shortest path. Due to the water solubility of dye particles, the path can be visualized and all possible paths can be explored.

EXPERIMENTAL SECTION

We investigated maze solving in mazes with different complexities made from poly(dimethylsiloxane) (PDMS) that were designed by photolithography and laser lithography. The channel was 1.4 mm thick and 1.0 mm deep. In experiments, we first filled the maze with an aqueous solution of KOH (Sigma-Aldrich, 0.05 M) containing 0.2 vol % 2-hexyldecanoic acid (Sigma-Aldrich) (2-HDA). A small block of agarose gel (Sigma-Aldrich) soaked in a solution of HCl (Sigma-Aldrich, 1.0 M) was placed at one entrance (exit) of the maze. Immediately after the addition of the acidic block, a small amount (~0.3 mg) of phenol red dye powder was placed at the liquid−air interface at the other entrance to the maze. The dye particles located at the interface moved toward regions of lower pH, that is, toward the

Received: May 15, 2014
Revised: June 17, 2014
Published: June 24, 2014

   dx.doi.org/10.1021/la5018467 | Langmuir 2014, 30, 9251−9255

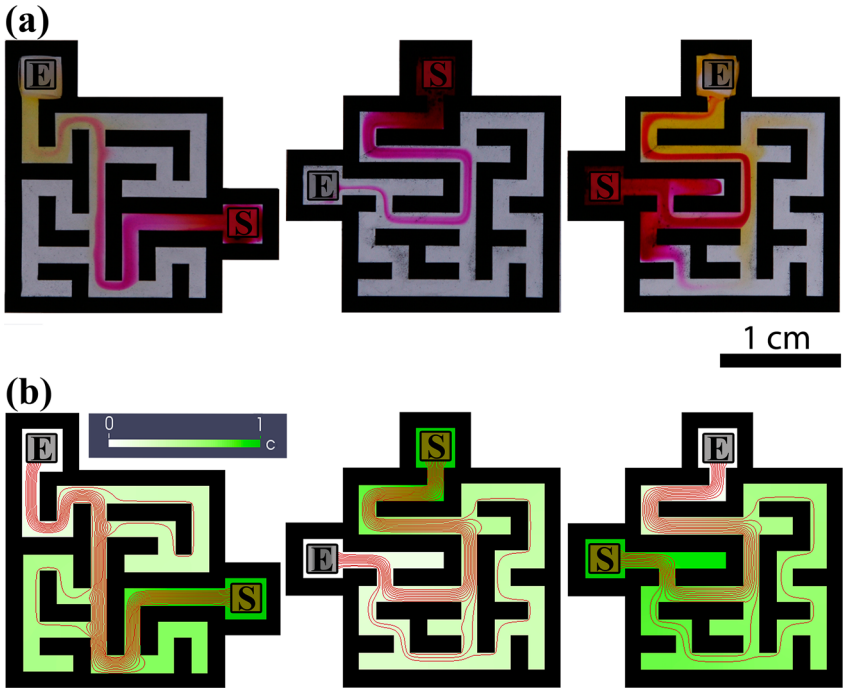

Figure 1. (a) Maze solving and finding the shortest paths in mazes filled with an alkaline solution of 2-hexyldecanoic acid. The position of the gel soaked with acid at the exit of the mazes is indicated by the letter E. The letter S shows the entrances of the maze, where phenol red dye particles are added. Marangoni flow induced by the pH gradient carries particles toward the acidic region at the liquid−air interface, and the shortest path is explored and visualized due to the water solubility of the dye. The yellow color near the exit originates from the color change of phenol red dye. Phenol red dye is red in alkaline solutions (pH >8.2) and yellow in acidic (pH <6.8) solutions. (b) Visualization of the shortest paths by streamlines that follow the highest concentration gradient in mazes. The stationary concentration distribution was calculated using the diffusion equation with $c = 1$ (at the entrance) and $c = 0$ (at the exit). This corresponds to the concentration of the deprotonated form of the 2-hexyldecanoic acid that is high at the entrance (basic medium) and low at the exit (acidic medium).

source of HCl. During transport, the dye particles dissolved in the liquid phase in the maze, thus exhibiting the path of those particles.

MODELING

In order to model this phenomenon, namely, the fluid flow in a 2D cross section in a channel, we considered the fully developed, steady flow within the 2D rectangular domain $\Omega \subset \mathbb{R}^2$ driven by a spatially nonuniform surface tension, γ, at the liquid−air interface. The fluid flow within the domain is described by the nondimensionalized Navier−Stokes equation[22]

$$\partial_t \mathbf{u} + \mathbf{u}\cdot\nabla\mathbf{u} = -\nabla p + Re^{-1}\Delta\mathbf{u}, \qquad \nabla\cdot\mathbf{u} = 0 \tag{1}$$

where $\mathbf{u} = (u_x(x, y), u_y(x, y))$ is the 2D velocity field and $Re = UL/\nu$ is the Reynolds number with a characteristic horizontal length L and velocity U and a dynamic viscosity ν. The Reynolds number can be interpreted as a measure of the importance of advection against the diffusion of the (linear) momentum of the fluid in the dynamics. The Marangoni-type flow considered here is driven by the nonuniform surface tension on the top (liquid−air) boundary (assumed rigid) which leads to the following constraints on the tangential stresses[23]

$$\frac{\partial u_x}{\partial y} = \frac{\partial \hat{\gamma}}{\partial x}, \qquad u_y = 0 \tag{2}$$

where $\hat{\gamma}$ is the dimensionless surface tension and the boundary is decomposed as $\partial\Omega \equiv \partial\Omega_T \cup \partial\tilde{\Omega}$, where $\partial\Omega_T$ denotes the top surface and $\partial\tilde{\Omega} = \partial\Omega/\partial\Omega_T$; the remaining boundary conditions are no-slip, i.e., $\mathbf{u}(x, y) = 0$ on $\partial\tilde{\Omega}$. By taking advantage of the 2D approximation, we can represent eq 1 as

$$\frac{\partial\nabla^2\psi}{\partial t} + \frac{\partial(\nabla^2\psi, \psi)}{\partial(x, y)} = Re^{-1}\nabla^4\psi \tag{3}$$

where the scalar stream function, ψ, is related to the velocity via $\mathbf{u} = (\partial_y\psi, -\partial_x\psi)$, $\partial(\nabla^2\psi, \psi)/\partial(x, y) \equiv \partial_x\nabla^2\psi\partial_y\psi - \partial_y\nabla^2\psi\partial_x\psi$ with $\partial_x \equiv \partial/\partial x$, $\partial_y \equiv \partial/\partial y$. In the stream-function representation, the boundary conditions become

$$\psi = 0 \text{ on } \partial\Omega, \qquad \mathbf{n}_{\partial\tilde{\Omega}}\cdot\nabla\psi = 0 \text{ on } \partial\tilde{\Omega}, \qquad \text{and} \qquad \partial_y{}^2\psi = \partial_x\hat{\gamma} \text{ on } \partial\Omega_T \tag{4}$$

We look for a fully developed steady solution of eq 3 which satisfies

$$\frac{\partial(\nabla^2\psi, \psi)}{\partial(x, y)} = Re^{-1}\nabla^4\psi \tag{5}$$

with the same boundary conditions as in eq 4. The numerical solutions to the nonlinear problem (eqs 4 and 5) are found by using a simple second-order, finite-difference discretization on a structured, equidistant grid which is combined with the Newton−Raphson iteration in order to find the solution; the biharmonic term, $\nabla^4\psi$, in eq 5 is discretized using the 13-point stencil, and the Laplacian in eq 5 is discretized using the standard 9-point stencil. We assume that the surface tension at the liquid−air interface can be approximated by the following functional form (Figure 2a)

dx.doi.org/10.1021/la5018467 | Langmuir 2014, 30, 9251−9255

$$\hat{\gamma} = \frac{\tanh(a(x - x_0))}{\tanh\left(a\left(\frac{1}{2} - x_0\right)\right) + \tanh\left(a\left(\frac{1}{2} + x_0\right)\right)} \quad (6)$$

where a and x_0 are constants. We can use this approximation, because the surface tension is determined by the concentration of deprotonated 2-HDA. This depends on pH, and in our experimental setup, the distribution of the pH (H^+) has a sigmoidal shape because an acidic source continuously releases H^+ ions into an alkaline solution (where the concentration of H^+ is low). In alkaline solution, the amount of the deprotonated form dominates, providing a lower surface tension compared to the surface tension in an acidic solution, in which the protonated form predominantly exists and the protonated form is insoluble in water. In other words, the distribution of pH translates into the distribution of surface tension. We should point out that obtaining a more precise distribution of the surface tension would involve solving a set of coupled reaction−diffusion−convection equations for all species. This complicates the model and its numerical solution. Our aim was to reproduce the main behavior observed in experiments, so we use eq 5 as a first approximation to estimate the surface tension profile at the liquid−air interface.

RESULTS AND DISCUSSION

Figure 1a shows the Marangoni flow-induced maze solving using various mazes with different entrance and exit locations. In these mazes with relatively simple topology, the shortest path can be visualized within ∼10 s using water-soluble dye particles. Maze solving by particles can be explained by surface tension originating from the nonuniform distribution of the deprotonated form of 2-HDA at the liquid−air interface. Initially the maze is filled with an alkaline solution, and 2-HDA molecules are homogeneously distributed and deprotonated at the liquid−air interface. By introducing an acidic block on one side, H^+ ions diffuse from the block, establishing a pH gradient that nonuniformly protonates the fatty acid molecules according to a reversible pH-dependent reaction $H^+ + DA^- \rightleftharpoons HDA$, where DA^- and HDA are the deprotonated and protonated forms of 2-HDA, respectively. Due to this reversible reaction the pH directly determines the concentration of the protonated and deprotonated forms of 2-HDA.[24] Importantly, less deprotonated 2-HDA is found in the direction facing the source of acid (i.e., toward lower pH). This asymmetric distribution translates into a gradient of surface tension which is determined predominantly by the concentration of the deprotonated 2-HDA at the liquid−air interface. The surface tension gradient gives rise to convective flow (toward low pH at the interface and opposite flow at the bottom of the channel, Figure 2a and Movie 1 in Supporting Information), which is ultimately responsible for particle motion, thus exhibiting the shortest path.

Figure 2 presents the generated convection roll in a channel (cross section) obtained from experiment and numerical simulation maintained by the Marangoni flow due to the inhomogeneous distribution of the deprotonated HDA at the interface. In experiments, we observed that the average velocity of a small tracer particle (here we used a small piece of PDMS of size 1.0 × 0.5 × 0.5 mm^3) is ∼1.3 mm/s (Figure 2a and Movie 1 in Supporting Information). However, it should be mentioned that the velocity of a tracer at the liquid−air interface is lower when further away from the acidic block. When it flows closer and approaches the acidic block because of convection, the velocity increases up to a maximum value (∼3 mm/s). The simplified numerical model also captures this behavior.

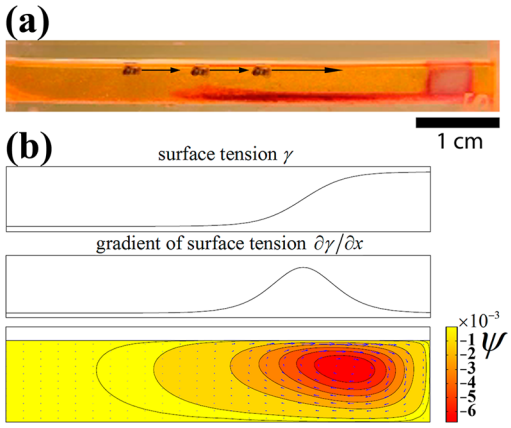

Figure 2. (a) Experimentally observed Marangoni flow induced by an acidic gel block in a narrow channel (thickness of 2 mm) containing an alkaline solution of 2-hexyldecanoic acid. Acid diffusing from the gel creates a pH gradient at the liquid−air interface that changes the concentration of the deprotonated 2-hexyldecanoic acid. This results in a surface tension difference and generates fluid flow toward lower-pH region at the interface. This flow carries a small piece of PDMS (1.0 × 0.5 × 0.5 mm^3) at the liquid−air interface. We added pH-neutral red dye for the visualization of the fluid flow in the medium. Video 1 accompanying the figure is included in the SI. (b) Simulated Marangoni flow by numerically solving the Navier−Stokes equation using a preexisting surface tension at the liquid−air interface (eq 5 in the text) with Re = 800, a = 10, and x_0 = 0.2. The values of the dimensionless surface tension are between 0.1 and 1.1.

Simulating the transport of passive tracer particles through the maze would involve solving the Navier−Stokes equation in 3D (eq 1, describing the velocity field) and convection−reaction−diffusion equations (describing the spatial variation of the protonated and deprotonated forms of 2-HDA and pH (H^+) equipped with an equation $\gamma = \gamma(DA^-)$ that determines the surface tension dependence on the deprotonated form of 2-HDA). Instead of carrying out these complicated (due to the geometry of the domain and boundary conditions) and time-consuming (due to 3D representation) numerical simulations, we can assume that the shortest path and all other possible paths through a maze can be obtained by drawing the streamlines of the gradient vector field of the concentration (which correlate with the highest surface tension gradient at a given point) at the liquid−air interface in a network of channels in 2D via solving the Laplace equation $\nabla^2 c = 0$, where c is the concentration of DA^-. Particles move toward the highest surface tension gradient that is equivalent to the highest concentration gradient, and thus each path can be represented as a streamline of the concentration gradient field. The concentration of the deprotonated form in a maze monotonically decreases with respect to a path length from a starting point (entrance of the maze). The stationary concentration distribution in a maze was calculated using the finite difference method on a rectangular mesh. The boundary conditions were the Neumann no-flux conditions for the wall of the maze and the Dirichlet conditions for the entrance and exit of the maze. For simplicity we used c = 1 at the entrance and c = 0 at the exit, which represent high and very low (virtually zero) concentrations of DA^- at the entrance and at the exit, respectively. Figure 1b shows the obtained streamlines from the

dx.doi.org/10.1021/la5018467 | Langmuir 2014, 30, 9251−9255

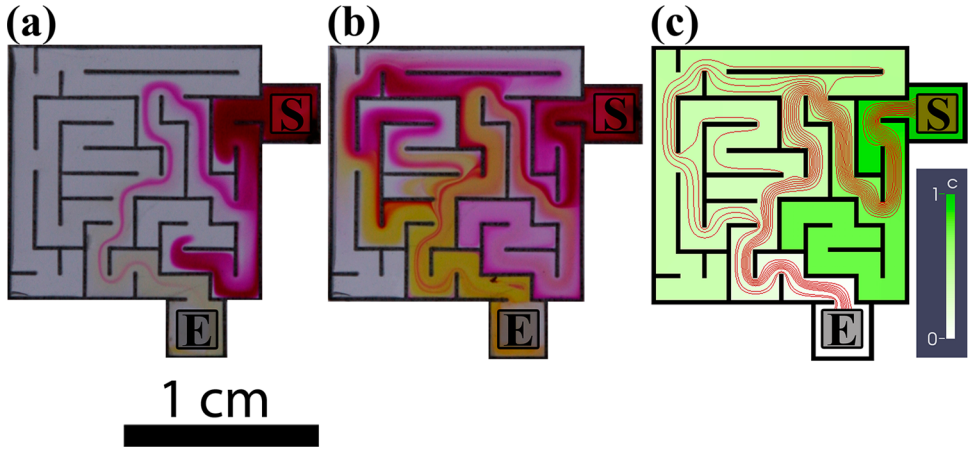

Figure 3. (a) Maze solving and finding the shortest path by phenol red dye particles after ∼10 s in a maze filled with an alkaline solution of 2-hexyldecanoic acid. (b) All possible paths can also be explored and can be fully visualized after ∼60 s. The position of the gel soaked with acid at the exit of the mazes is indicated by the letter E. The letter S shows the entrances of the maze, where dye particles are added. (c) Visualization of the shortest path and all possible paths by streamlines that follow the highest concentration gradient in mazes.

numerical simulations, where it can be seen that most of these streamlines follow the shortest paths in various mazes, thus solving the maze problem.

Importantly, in our experiments the particles always find the shortest path through the maze; however, with increasing time, longer alternative paths are also found. Figure 3 presents this situation in a topologically more complex maze than presented in Figure 1. Figure 3a shows the visualized shortest path in a maze after ∼10 s. There are always several streams in channels in the maze connected and interconnected with the acidic block (exit) that maintain the fluid flow. The intensity of these streams is inversely proportional to the length of the paths. In other words, the most intense fluid flow is established along a path in a maze, where the gradient of the surface tension at the liquid−air interface is the highest. Therefore, the most intense stream is realized in the shortest path that carries most of the dye particles, thus the shortest path is visualized at first. Less intense flow can carry fewer particles; therefore, the visualization of longer paths needs proportionally more time. However, eventually all possible paths would be explored and visualized due to the dissolution of solid dye particles (Figure 3b,c). It should also be mentioned that some dye particles can migrate into dead-end channels (Figures 1a and 3a). This could be attributed to the fact that the generated fluid flow in a maze can induce some fluid motion in those channels in which no surface tension gradient is established due to the inertia of the fluid flow.

To illustrate our maze-finding concept in a realistic configuration, we fabricated a maze by analogy to the street map of downtown Budapest (Figure 4). In this setup, similar to that in former experiments, we filled the maze with an alkaline solution of 2-HDA and added a solid hydrogel block soaked with acid to the end point (the place to find is indicated by B in Figure 4). After that we added a small amount of phenol red dye powder to the starting point (indicated by A in Figure 4). The shortest path was visualized within 60 s, as in our previous setups due to induced Marangoni flow.

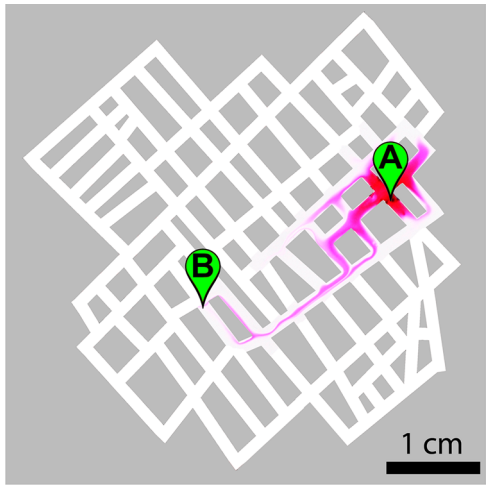

Figure 4. Finding the shortest path between two points in a channel network (made from PDMS) based on the street map of downtown Budapest filled with an alkaline solution of 2-hexyldecanoic acid. The position of the gel soaked with acid (end point) is indicated by the letter B. The letter A shows the starting point, where phenol red dye particles are added.

■ CONCLUSIONS

We have shown a simple method for maze solving and visualizing all possible paths using fatty acid chemistry. Contrary to a previous study,[11] in which a chemotactic fatty acid droplet could solve the maze finding the shortest path due to releasing a surface-active compound and creating its own convective flow in a pH gradient that is responsible for the motion of the droplet,[25,26] here we described a system where the dye particles can move passively toward lower pH at the liquid−air interface due to generated Marangoni flow. Meanwhile, these particles dissolve into a liquid phase and show the visualized solutions in a maze. Our system also differs from the maze-solving method described in ref 10, in which a submerged polymer hydrogel in a bulk liquid phase can find the shortest path in a microfluidic maze driven by the liquid-mixing-induced Marangoni effect. Our method is based on a nonlocal approach as opposed to the local algorithms which must use either some stochastic kicks to get out of the local minima or the wall-following algorithms, which are extremely slow. The global approach requires a knowledge of the topology of the maze, which is often unrealistic. Here this problem can be overcome by exploiting information from a globally imposed field. This

dx.doi.org/10.1021/la5018467 | *Langmuir* 2014, 30, 9251−9255

unconventional computational approach provides a flexible way to explore not only the shortest path but also all existing paths in parallel through a maze. A further advantage of this method is that the process is fast compared to other chemical-based computing methods and can also show the paths, so additional postprocessing techniques are not required.

■ ASSOCIATED CONTENT

Supporting Information

Movie showing the generated Marangoni flow induced by an acidic gel block in a narrow channel (thickness of 2 mm) containing the alkaline solution of a fatty acid. This material is available free of charge via the Internet at http://pubs.acs.org.

■ AUTHOR INFORMATION

Corresponding Author

*E-mail: lagzi@vuk.chem.elte.hu. Tel: +361-463-1341. Fax: +361-463-4180.

Notes

The authors declare no competing financial interest.

■ ACKNOWLEDGMENTS

We acknowledge the financial support of the Hungarian Research Fund (OTKA K104666) and JSPS KAKENHI (grant number 23540165). Financial support by the Swiss National Science Foundation under project 200021-137868 is gratefully acknowledged. R.T. is grateful for financial support from the Marie-Heim-Vögtlin Foundation under project number PMPDP2-139698.

■ REFERENCES

(1) Adamatzky, A. I. Computation of Shortest Path in Cellular Automata. *Math. Comput. Modelling* **1996**, *23*, 105−113.
(2) Dijkstra, E. N. A Note on Two Problems in Connexion with Graphs. *Numer. Math.* **1959**, *1*, 269−271.
(3) Fuerstman, M. J.; Deschatelets, P.; Kane, R.; Schwartz, A.; Kenis, P. J. A.; Deutch, J. M.; Whitesides, G. M. Solving Mazes Using Microfluidic Networks. *Langmuir* **2003**, *19*, 4714−4722.
(4) Steinbock, O.; Tóth, A.; Showalter, K. Navigating Complex Labyrinths: Optimal Paths from Chemical Waves. *Science* **1995**, *267*, 868−871.
(5) Reyes, D. R.; Ghanem, M. M.; Whitesides, G. M.; Manz, A. Glow Discharge in Microfluidic Chips for Visible Analog Computing. *Lab Chip* **2002**, *2*, 113−116.
(6) Pershin, Y. V.; Di Ventra, M. Solving Mazes with Memristors: A Massively Parallel Approach. *Phys. Rev. E* **2011**, *84*, 046703.
(7) Nakagaki, T.; Yamada, H.; Tóth, A. Intelligence: Maze-solving by an Amoeboid Organism. *Nature* **2000**, *407*, 470−470.
(8) Nakagaki, T.; Yamada, H.; Tóth, A. Path Finding by Tube Morphogenesis in an Amoeboid Organism. *Biophys. Chem.* **2001**, *92*, 47−52.
(9) Adamatzky, A. Physarum Machines for Space Missions. *Acta Futura* **2013**, *6*, 53−67.
(10) Wang, Y.; Liu, X.; Li, X.; Wu, J.; Long, Y.; Zhao, N.; Xu, J. Directional and Path-Finding Motion of Polymer Hydrogels Driven by Liquid Mixing. *Langmuir* **2012**, *28*, 11276−11280.
(11) Lagzi, I.; Soh, S.; Wesson, P. J.; Browne, K. P.; Grzybowski, B. A. Maze Solving by Chemotactic Droplets. *J. Am. Chem. Soc.* **2010**, *132*, 1198−1199.
(12) Adamatzky, A. Slime Mold Solves Maze in One Pass, Assisted by Gradient of Chemo-Attractants. *IEEE Trans. Nanobiosci.* **2012**, *11*, 131−134.
(13) Scriven, L. E.; Sternling, C. V. The Marangoni Effects. *Nature* **1960**, *167*, 186−188.
(14) Sawistowski, H. Influence of Mass-Transfer-Induced Marangoni Effects on Magnitude of Interfacial Area and Equipment Performance in Mass Transfer Operations. *Chem. Ing. Techn.* **1973**, *43*, 1114−1117.
(15) Tseng, Y. T.; Tseng, F. G.; Chen, Y. F.; Chieng, C. C. Fundamental Studies on Micro-Droplet Movement by Marangoni and Capillary Effects. *Sens. Actuators A* **2004**, *114*, 292−301.
(16) Pesach, D.; Marmur, A. Marangoni Effects in the Spreading of Liquid Mixtures on a Solid. *Langmuir* **1987**, *3*, 519−524.
(17) Tadmor, R. Marangoni Flow Revisited. *J. Colloid Interface Sci.* **2009**, *332*, 451−454.
(18) Tadmor, R. Drops That Pull Themselves Up. *Surf. Sci.* **2014**, *628*, 17−20.
(19) Bliznyuk, O.; Jansen, H. P.; Kooij, E. S.; Zandvliet, H. J. W.; Poelsema, B. Smart Design of Stripe-Patterned Gradient Surfaces to Control Droplet Motion. *Langmuir* **2011**, *27*, 11238−11245.
(20) Rongy, L.; De Wit, A. Steady Marangoni Flow Traveling with Chemical Fronts. *J. Chem. Phys.* **2006**, *124*, 164705.
(21) Jensen, O. E. Self-similar, Surfactant-Driven Flows. *Phys. Fluids* **1994**, *6*, 1084−1094.
(22) Bragard, J.; Velarde, M. G. Benard-Marangoni Convection: Planforms and Related Theoretical Predictions. *J. Fluid Mech.* **1998**, *368*, 165−194.
(23) Batchelor, G. K. *An Introduction to Fluid Dynamics*; Cambridge University Press: Cambridge, U.K., 1967.
(24) Schramm, L. L.; Stasiuk, E. N.; Marangoni, D. G. Surfactants and Their Applications. *Annu. Rep. Prog. Chem., Sect. C: Phys. Chem.* **2003**, *99*, 3−48.
(25) Reynolds, A. M. Maze-solving by chemotaxis. *Phys. Rev. E* **2010**, *81*, 062901.
(26) Grancic, P.; Stepanek, F. Swarming Behavior of Gradient-Responsive Brownian Particles in a Porous Medium. *Phys. Rev. E* **2012**, *86*, 011916.